Electronic Supplementary Information to the paper entitled: "Calcite surface structure and reactivity: molecular dynamics simulations and macroscopic surface modelling of the calcite-water interface" by M. Wolthers, D. Di Tommaso, Z. Du and N.H de Leeuw

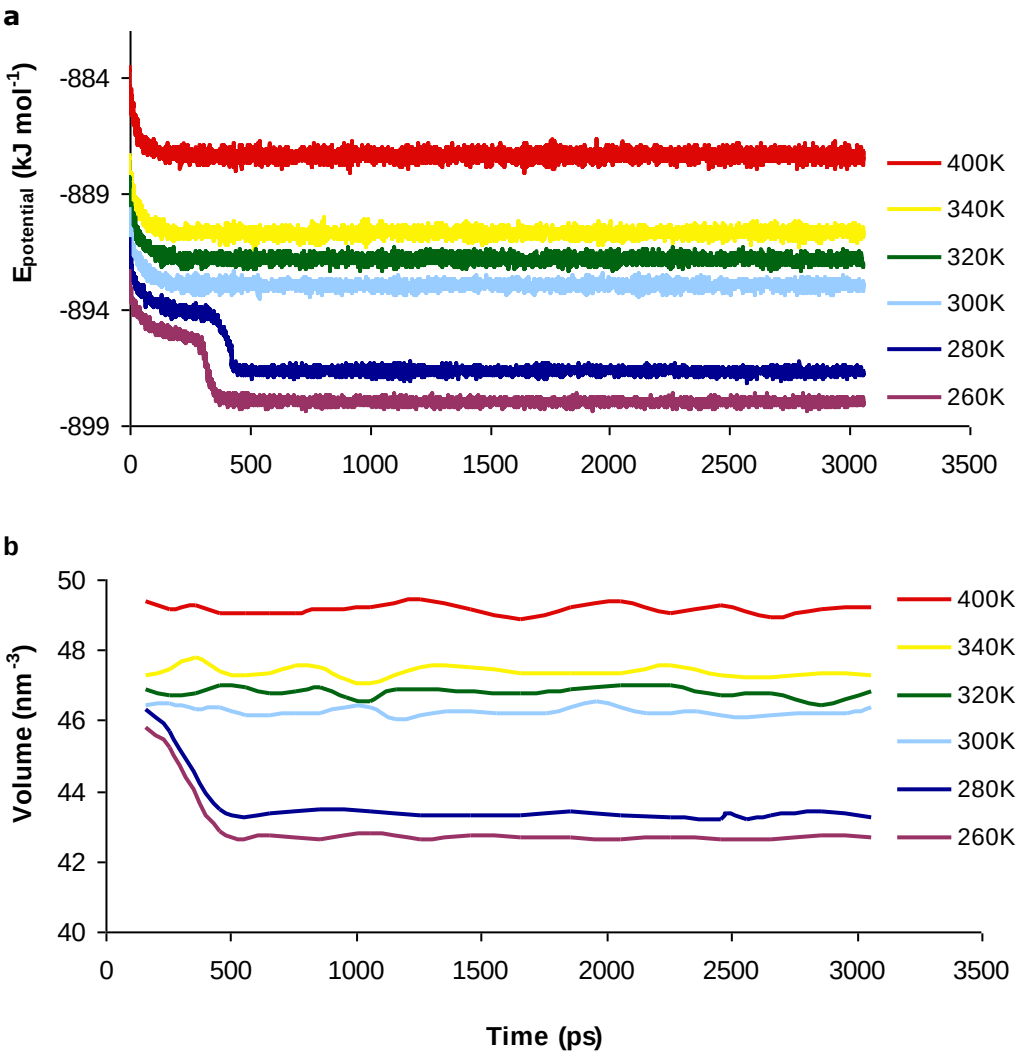

Figure S1. (A) Potential energy and (B) volume for 2028 water molecules at six different temperatures during NPT production. Within 500 ps of production, a phase change is observed for water at 260K and 280K.

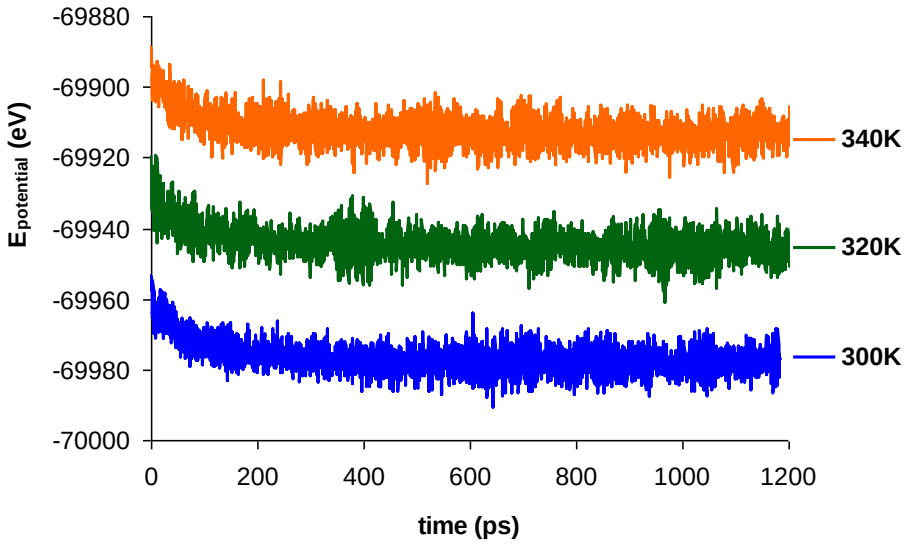

Figure S2. Potential energy for calcite slab (840 $CaCO_3$) with water layer (2048 H_2O; density ρ = 1.21 g/cm^3 at 300K[Error! Reference source not found.]) during production in NPT at different temperatures.

Table S1. Potential parameters used in this work (short-range cut-off 8.0 Å).

Charges (e)			**Core-shell interaction (eV Å^{-2})**
Ion	**Core**	**Shell**	
Ca	+2.000		
C	+1.135		
H	+0.400		
Carbonate oxygen (O)	+0.587	−1.632	507.400000
Water oxygen (O_{water})	+1.250	−2.050	209.449602
		Buckingham potential	
Ion pair	A (eV)	ρ (Å)	C (eV Å^6)
Ca−O	1550.0	0.29700	0.0
Ca−O_{water}	1186.6	0.29700	0.0
H−O	396.3	0.23000	0.0
H−O_{water}	396.3	0.23000	10.0
O−O	16,372.0	0.21300	3.47
O−O_{water}	12,533.6	0.21300	12.09
C−O_{water}	435.0	0.34370	0.0
		Lennard-Jones potential	
	A (eV Å^{12})		B (eV Å^6)
O_{water}−O_{water}	39344.98		42.15
		Morse potential	
	D (eV)	A (Å^{-1})	r_0 (Å)
C−O	4.710000	3.80000	1.18000
H−O_{water}	6.203713	2.22003	0.92376
H−H	0	2.840499	1.5
		Three-body potential	
	k (eV rad^{-2})		Θ_0
O_{core}−C−O_{core}	1.69000		120.000000
H−$O_{water,\ shell}$−H	4.19978		108.693195
		Four-body potential	
	k (eV rad^{-2})		Θ_0
C−O_{core}−O_{core}−O_{core}	0.11290		180.0
		Coulombic subtraction (%)	
$H^{0.4+}$−$O^{0.8-}$		50	
$H^{0.4+}$−$H^{0.4+}$		50	

Table S2. Distribution of the number of hydrogen-bonds for the water molecules coordinated to the different calcium surface sites. The values given are percentages of molecules with the given number of hydrogen-bonds[Error! Reference source not found.]

		number of hydrogen-bonds							
	Ca^{2+} position	**0 (%)**	**1 (%)**	**2 (%)**	**3 (%)**	**4 (%)**	**5 (%)**	**6 (%)**	**average**
300K	Face site	2.2	19.8	42.7	27.4	7.1	0.8	0.1	2.20
	Acute edge site	3.1	23.6	39.2	24.6	7.9	1.5	0.2	2.16
	Obtuse edge site	2.1	17.4	42.2	28.1	8.9	1.2	0.1	2.28
	Acute corner site	2.2	19.8	42.7	27.4	7.1	0.8	0.1	2.20
	Obtuse corner site	3.9	23.6	39.1	24.3	7.8	1.1	0.2	2.13
320K	Face site	2.6	20.1	42.4	27.1	7.0	0.75		2.18
	Acute edge site	4.0	23.3	38.0	24.1	8.5	1.5		2.16
	Obtuse edge site	2.6	18.6	40.1	28.5	9.1	1.2		2.27
	Acute corner site	2.7	19.4	41.1	27.1	8.3	1.3		2.24
	Obtuse corner site	3.2	22.5	40.4	25.4	7.4	1.2		2.15
340K	Face site	2.9	21.1	42.1	26.2	6.8	0.8		2.16
	Acute edge site	4.1	24.2	30.5	24.7	8.1	1.3		2.13
	Obtuse edge site	2.9	20.4	40.0	27.0	8.1	1.3		2.22
	Acute corner site	2.5	22.1	40.3	26.0	8.0	1.1		2.19
	Obtuse corner site	3.5	23.9	39.6	23.8	8.1	1.1		2.13

Table S3. Distribution of the number of hydrogen-bonds[56] for oxygen within surface carbonate groups at structurally different positions.

		number of hydrogen-bonds							
	CO_3^{2-} position	**0 (%)**	**1(%)**	**2 (%)**	**3 (%)**	**4 (%)**	**5 (%)**	**6 (%)**	**average**
300K	Face (A)	34.4	55.6	9.8	0.2	0.0	0.0	0.0	0.73
	Face (X)	60.9	34.2	4.8	0.1	0.0	0.0	0.0	0.30
	Face (B)	51.9	42.1	5.9	0.1	0.0	0.0	0.0	0.20
	Acute edge (A)	21.1	44.9	24.9	7.5	1.5	0.1	0.0	1.29
	Acute edge (X)	33.9	40.1	20.1	5.5	0.4	0.0	0.0	0.95
	Acute edge (B)	48.0	46.8	4.9	0.2	0.0	0.0	0.0	0.42
	Obtuse edge (A)	34.9	39.2	15.6	7.7	2.6	0.2	0.0	1.02
	Obtuse edge (X)	17.2	52.9	22.3	6.6	0.9	0.0	0.0	1.34
	Obtuse edge (B)	62.1	32.9	4.8	0.2	0.0	0.0	0.0	0.30
	Acute corner (A)	21.4	50.4	23.2	4.7	0.4	0.0	0.0	1.53
	Acute corner (X)	19.2	42.0	31.6	6.7	0.6	0.0	0.0	1.79
	Acute corner (B)	23.9	43.8	25.6	6.0	0.6	0.1	0.0	0.75
320K	Face (A)	32.0	57.9	9.9	0.2	0.0	0.0	0.0	0.82
	Face (X)	65.9	31.9	3.7	0.1	0.0	0.0	0.0	0.26
	Face (B)	52.6	41.0	6.3	0.2	0.0	0.0	0.0	0.16
	Acute edge (A)	24.6	49.1	19.8	5.5	1.0	0.8	0.0	1.43
	Acute edge (X)	34.8	36.5	22.5	5.9	0.5	0.0	0.0	0.82
	Acute edge (B)	58.3	39.8	1.9	0.0	0.0	0.0	0.0	0.33
	Obtuse edge (A)	35.7	40.2	15.7	6.7	1.8	0.2	0.0	1.20
	Obtuse edge (X)	27.7	46.1	20.0	5.6	0.7	0.0	0.0	1.24
	Obtuse edge (B)	70.2	28.2	1.7	0.1	0.0	0.0	0.0	0.24
	Acute corner (A)	26.2	46.5	22.0	4.9	0.5	0.0	0.0	1.54
	Acute corner (X)	18.9	46.7	29.6	4.8	0.1	0.0	0.0	1.61
	Acute corner (B)	22.4	51.2	21.4	4.7	0.5	0.0	0.0	0.65
340K	Face (A)	40.4	50.7	8.4	2.8	0.1	0.0	0.0	0.58
	Face (X)	60.0	35.3	4.7	0.1	0.0	0.0	0.0	0.27
	Face (B)	44.5	47.6	7.7	0.2	0.0	0.0		0.36
	Acute edge (A)	34.2	42.1	20.3	3.2	0.1	0.0	0.0	0.73
	Acute edge (X)	24.3	45.6	21.5	7.4	1.0	0.2	0.0	1.48
	Acute edge (B)	46.4	49.2	4.1	0.3	0.0	0.0	0.0	0.39
	Obtuse edge (A)	30.8	38.1	19.8	9.0	2.2	0.1	0.0	1.12
	Obtuse edge (X)	31.5	42.2	18.2	6.8	1.3	0.1	0.0	0.92
	Obtuse edge (B)	35.8	53.2	10.4	0.5	0.0	0.0	0.0	0.62
	Acute corner (A)	21.2	47.6	25.5	5.4	0.4	0.0	0.0	1.53
	Acute corner (X)	16.2	49.2	29.3	5.0	0.3	0.0	0.0	1.54
	Acute corner (B)	25.4	50.6	19.2	4.2	0.7	0.0	0.0	0.61